

**MASSACHUSETTS INSTITUTE OF TECHNOLOGY
DEPARTMENT OF MECHANICAL ENGINEERING
CAMBRIDGE, MASSACHUSETTS 02139**

**2.002 MECHANICS and MATERIALS II
SPRING 2004**

SUPPLEMENTARY NOTES

© L. Anand and D. M. Parks

DEFECT-FREE FATIGUE

1. INTRODUCTION

Fatigue Failure is the failure of components under the action of repeated fluctuating stresses or strains. The word “fatigue” was introduced in the 1840’s and 1850’s in connection with such failures which occurred in the then rapidly developing railway industry. It was found that railroad axles failed regularly at shoulders, and that these failures appeared to be quite different from failures associated with monotonic testing.

Fatigue failure may be defined as a process in which there is progressive, localized, permanent microstructural change occurring in a structure when it is subjected to boundary conditions which produce fluctuating stresses and strains at some material point or points. These microstructural changes may culminate in the formation of cracks and their subsequent growth to a size which causes final fracture after a sufficient number of stress or strain fluctuations.

The adjective “**progressive**” implies that the fatigue process occurs over a period of time or usage. The occurrence of a fatigue failure is often very sudden, with no external warning; however, the mechanisms involved may have been operating since the beginning of the time when the component or structure was put to use.

The adjective “**localized**” implies that the fatigue process operates preferentially at specific local areas, rather than homogeneously throughout the body. These vulnerable areas can have high local strains and stresses due to stress and strain concentrations caused abrupt changes in geometry and/or material imperfections.

The phrase “**permanent microstructural changes**” emphasizes the central role of cyclic plastic deformations in causing irreversible changes in the substructure. Countless investigations have established that **fatigue results from cyclic plastic deformation in every instance**, even though the structure as a whole is practically elastic. A small plastic strain excursion applied only once does not cause any substantial changes in the substructure of materials, but multiple repetitions of very small plastic strains lead to cumulative damage ending in fatigue failure. We note that although fatigue is popularly associated with metallic materials, it can occur in all engineering materials capable of undergoing plastic deformation. This includes polymers, and composite materials with plastically deformable phases. Plastically non-deformable materials such as glasses and ceramics, in which deformations at ambient temperatures are truly elastic everywhere, do not fail by fatigue due to repeated stresses. However, recent data has shown that polycrystalline ceramics can exhibit fatigue crack growth under certain circumstances. Such a process is still consistent with our definition in the sense that local irreversible deformation at the crack tip associated with processes such as microcracking, frictional sliding, particle detachment and crack face wedging are involved in the fatigue process. Furthermore, these local mechanisms in brittle materials can give rise to macroscopic

behavior which is phenomenologically similar to plasticity.

There are currently two principal methodologies for design and maintenance to resist fatigue failure of components, **defect-free** and **defect-tolerant**. These two approaches are based on the how the crack size a in a component increases with the number of stress or strain cycles N imposed on the component.

1. DEFECT-FREE DESIGN AND MAINTENANCE APPROACH:

The defect-free approach is mostly used to design small components which are not safety critical.

In this approach, it is assumed that no crack-like defects pre-exist. That is, the initial crack size a is taken to be zero. Figure 1 shows a schematic of the behavior of crack size, a , versus the number of applied cycles of loading, N , for an initially uncracked component. The **number of cycles to fatigue failure** of the component is denoted by N_f (the subscript “ f ” here refers to “failure”). The total number of loading cycles to failure may be conceptually decomposed as

$$N_f = N_i + N_p, \tag{1}$$

where N_i is the **number of cycles required to initiate a fatigue crack**, and N_p is the **number of cycles required to propagate a crack to final fracture after it has initiated**. Of course, the precise boundary between these two regions depends on the value chosen for the “initiation” crack size, a_i .

Although the total fatigue life, within the defect-free approach, consists of an “initiation” life and a “propagation” life, fatigue “failure” is often said to have occurred when a crack has initiated. This simplification is adopted since usually $N_p \ll N_i$; in such case, the “propagation” life, N_p , can be neglected in comparison to the “initiation” life, N_i , and total fatigue life, N_f , is approximated as

$$N_f \approx N_i.$$

Further, a fatigue crack in a typical engineering component is often said to have “initiated” when it is readily visible to the naked eye, that is $a_i \approx 1$ mm. Of course, specific circumstances (e.g., “small” components) may require adoption of other, more appropriate, definitions of fatigue “initiation” and initiation crack size.

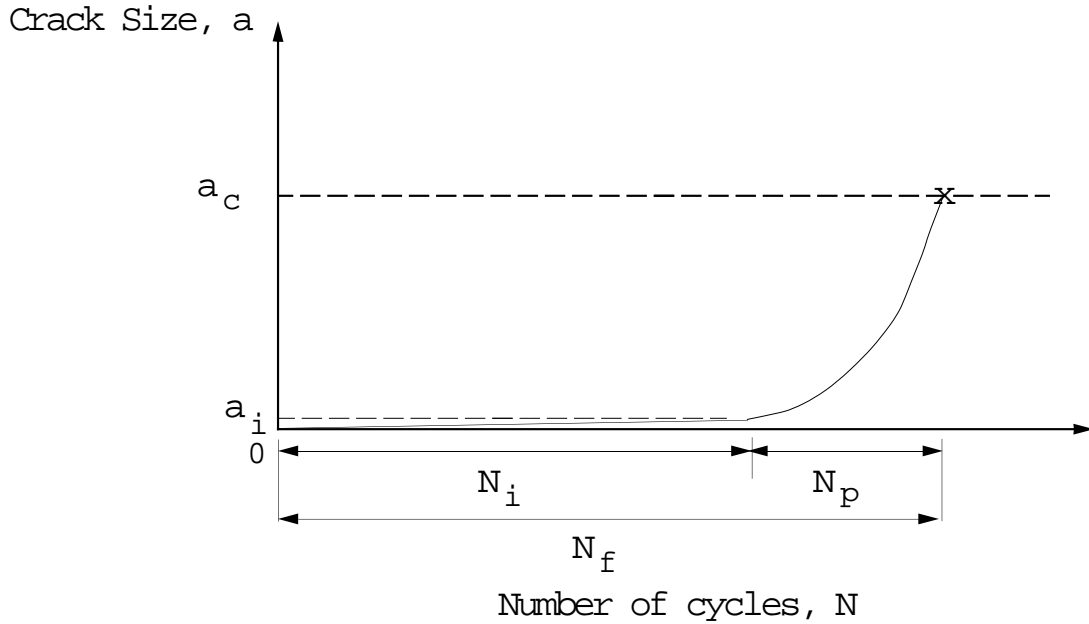


Figure 1: Schematic of crack length, a , versus number of loading cycles, N , in an initially uncracked component.

The defect-free methodology is usually sub-divided into two sub-categories.

(a) **High-cycle fatigue:**

High-cycle fatigue is associated with local cyclic stresses which are of sufficiently small magnitude so that they produce predominantly elastic straining, and the resulting fatigue life exceeds $\approx 10^4$ cycles.

Examples of components designed in consideration of high-cycle fatigue include most rotating and vibrating members.

(b) **Low-cycle fatigue:**

Low-cycle fatigue is associated with local cyclic stress levels which are sufficiently large so that significant cyclic plastic straining occurs, and the resulting fatigue life is less than $\approx 10^4$ cycles.

Example applications that are designed in consideration of low-cycle fatigue include core components of nuclear reactors and gas turbine engines, which in their lifetime may see a limited number of modestly large cyclic straining events associated with start-up and shut-down cycles. Other application areas include design of many ground vehicle components which are occasionally subjected to overloads sufficient to cause local yielding at notch roots, etc.

2. DEFECT-TOLERANT DESIGN AND MAINTENANCE APPROACH:

If the potential costs of a structural fatigue failure in terms of human life and dollars is very high, then the design of such engineering components and structures is often [more conservatively] based on:

- (a) The assumption that all fabricated components and structures contain a pre-existing population of cracks of an initial size a_i . This initial size should be taken to be the larger of (i) the largest actually-detected initial crack, and (ii) **the detection-limit crack size, a_d** , which is the largest crack size that can escape detection by the adopted non-destructive testing (NDT) method. Because it is assumed in this approach that a crack pre-exists, $N_i = 0$, and therefore $N_f = N_p$. See Figure 2.
- (b) The requirement that none of the population of assumed pre-existing cracks be permitted to grow to a critical size during the expected service life of the part or structure. Normally, this requires the selection of **inspection intervals** within the service life. In application of such defect-tolerant strategies, it is also assumed that the initial location and orientation of the [typically not actually detected] defect is the “worst possible”; that is, that it occurs at the point of highest cyclic stress, and is oriented perpendicular to the cyclic tensile stress range at that location.

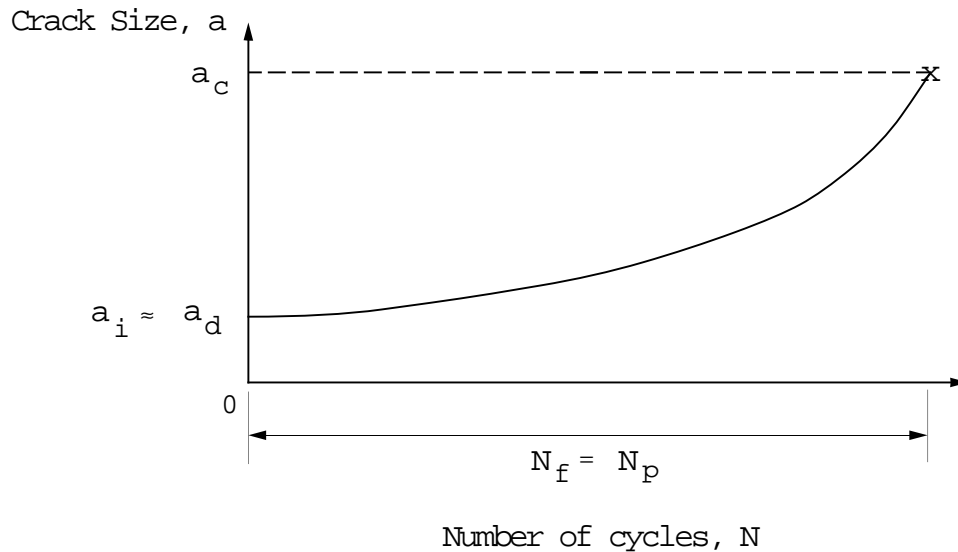


Figure 2: Schematic of crack length, a , versus number of cycles, N , in a component with an initial crack size a_i . The initial crack size is typically taken to be the largest crack size, a_d , that can escape detection by NDT techniques.

The major aim of the defect-tolerant approach to fatigue is to reliably predict

the growth of pre-existing cracks of specified initial size, a_i , shape, location, and orientation in a structure subjected to prescribed cyclic loadings. Providing this goal can be achieved, then inspection and service intervals can be established such that cracks should be readily detectable well before they have grown to near critical size, a_c .

The defect-tolerant approach to fatigue is typically used in the design and maintenance of large, fabricated structures such as aircraft, ships, pressure vessels, etc., where welds are likely sites for initial defects, and the large size of the components may permit substantial subcritical crack growth, so that the enlarged defect can be detected and repaired or replaced well before it reaches a critical dimension. Defect-tolerant strategies are also appropriate to safety-critical applications of components of arbitrary size.

Within the scope of a defect-tolerant approach, two sub-approaches may be identified. One of these is termed **fail-safe design**. In this case, the basic concept is that a structure should possess a sufficient redundancy of elements or components to provide assurance that, for a specified operating load, the failure or fracture of any single element or component will not lead to catastrophic failure of the structural assembly. The implementation of this approach may require a very high degree of conservatism in design.

A somewhat less conservative defect-tolerant approach may be termed **safe-life design and maintenance**. In this approach, the basic premise is that, in a specified operating interval (either total operating life, or, more commonly, an operating interval between scheduled shut-down, inspection, and maintenance procedures), no pre-existing crack of specified size, location, and orientation should grow to a size at which a specified load would cause the element containing the crack to fail.

In a previous handout, we have outlined major features of the defect-tolerant approach (see also, Dowling text, Chapter 12). In the following sections we discuss the experimental foundations on which the defect-free approach to design against fatigue failure is based, and outline some details of how the approach is actually implemented.

In practice, defect-free fatigue is characterized by three basic entities whose interactions and connections comprise the field. These three entities are:

1. the cyclic stress history at the critical location;
2. the corresponding history of cyclic strain, where the cyclic strain is, in general, the sum of both cyclic elastic and cyclic plastic parts; and
3. the number of cycles of the cyclic loading leading to the initiation of a representative “initiation crack size”, a_i ; within the defect-free methodology, this is equated with the fatigue failure life.

The pairwise connections between cyclic stresses and cyclic strains are summarized by a so-called **cyclic stress-strain relation**; functional forms for these connections will be similar to those connecting stress to elastic and plastic strain in monotonic tension, but material parameters entering the respective “cyclic” and “monotonic’ expressions will differ. In traditional high-cycle fatigue, experimental connections are made between the fatigue life and the cyclic stressing, including a stationary mean stress. Alternatively, an equivalent correlation for high-cycle fatigue could be made between fatigue life and the cyclic elastic strain. In low cycle fatigue, the fatigue life is robustly correlated with the cyclic plastic strain. Finally, using the cyclic stress/strain relations, we can combine high-cycle and low-cycle fatigue into a single, unifying correlation of fatigue life with [total] cyclic strain.

However, first we examine the similarities and differences between the monotonic and cyclic stress-strain response of materials.

Monotonic and Cyclic Stress-Strain Response:

We have already covered many aspects of the elastic-plastic behavior of polycrystalline metals subjected to monotonic uniaxial tensile loading and monotonic loading followed by elastic unloading. Under **cyclic** loading conditions the stress-strain response can differ from the monotonic response. In this sub-section we will develop **cyclic stress-strain relations** to describe this response. We shall see that the equations which describe cyclic response bear a strong similarity to those describing monotonic response, but with different independent and dependent variables and different values for the material parameters.

Monotonic Stress-Strain Behavior

A stress-strain curve for monotonic uniaxial tensile loading followed by an elastic unloading is shown schematically in Fig. 3. The total strain ϵ is the sum of the elastic strain, ϵ^e , plus plastic strain, ϵ^p :

$$\epsilon = \epsilon^e + \epsilon^p. \quad (2)$$

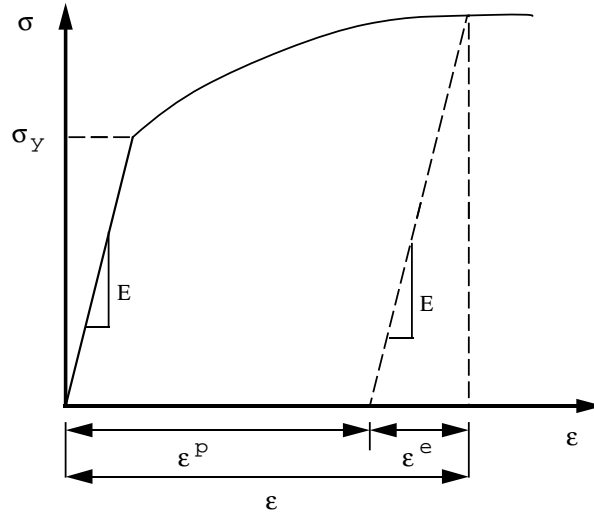


Figure 3: Schematic of stress-strain behavior for monotonic loading.

The constitutive assumption which relates the elastic strain to stress is

$$\epsilon^e = \frac{\sigma}{E}, \quad (3)$$

where E is Young's modulus, and σ is the stress. The plastic strain ϵ^p is negligibly small for stresses less than a certain value, σ_y , termed the initial **yield strength**. For higher values of σ , it is often found that a power law relation of the form

$$\epsilon^p = \left(\frac{\sigma}{K}\right)^{1/n} \quad \text{or} \quad \sigma = K(\epsilon^p)^n, \quad (4)$$

connects ϵ^p and σ very well for $\epsilon^p \geq .002$ or so. The dimensionless material parameter n is called the **strain hardening exponent**, with typical values $.01 < n \leq .4$, and the stress-dimensioned material parameter K is called the **strength coefficient**. Upon inserting equations (3, 4) into equation (2), we obtain

$$\boxed{\epsilon = \frac{\sigma}{E} + \left(\frac{\sigma}{K}\right)^{1/n}}. \quad (5)$$

This equation is often referred to as a **Ramberg-Osgood stress-strain relation**, in recognition of the early proponents of this phenomenological stress-strain relation.

It can be seen from equation (4) that the parameter (σ/K) is raised to a large power, $1/n$, and hence for $(\sigma/K) \ll 1$, the plastic strain is exceedingly small. Thus, there is often little error associated with the use of equation (5) even for stresses σ which are less than the initial yield strength, σ_y .

At the point of fracture in a tension test, the **true stress at fracture**, σ_f , is defined by

$$\sigma_f = \frac{P_f}{A_f}, \quad (6)$$

where P_f is the fracture load and A_f is the fracture surface area. The **true strain at fracture**, ϵ_f , (using the assumption of incompressibility) can be expressed as

$$\epsilon_f = \ln\left(\frac{A_0}{A_f}\right), \quad (7)$$

where A_0 is the initial cross-sectional area.

Since in ductile materials the plastic strain at fracture greatly exceeds the elastic strain, we may say that ϵ_f is essentially equal to the plastic strain at fracture. We can then substitute ϵ_f and σ_f into equation (4) to solve for K as

$$K = \frac{\sigma_f}{(\epsilon_f)^n}. \quad (8)$$

On substituting equation (8) into equation (5) we obtain

$$\epsilon = \frac{\sigma}{E} + \epsilon_f \left(\frac{\sigma}{\sigma_f} \right)^{1/n}. \quad (9)$$

The form (11) of the Ramberg-Osgood equation contains four material constants: E , σ_f , ϵ_f , and n .

The monotonic properties $\{E, \sigma_y, \sigma_{TS}, K, n, \sigma_f, \epsilon_f\}$ for some representative metallic materials are listed in Table 1. Recall that σ_{TS} is the ultimate tensile strength, which is determined as the maximum point in the engineering stress versus engineering strain curve obtained in a standard uniaxial tension test.

Material	Monotonic Properties							Cyclic Properties		
	E GPa	σ_y MPa	σ_{TS} MPa	K MPa	n	σ_f MPa	ϵ_f	σ'_y MPa	K' MPa	n'
Steel										
SAE 1020 (hot rolled)	206	262	441	738	0.19	710	0.96	241	772	0.18
SAE 1040 (As forged)	210	345	621	738	0.22	1050	0.93	386	786	0.18
Man-Ten (hot rolled)	203	322	557	738	0.2	814	1.02	372	786	0.11
RQC-100 (hot rolled)	200	883	931	1172	0.06	1330	1.02	600	1434	0.14
SAE 4340 (Q & T)	200	1172	1241	1579	0.066	1655	0.84	758	1434	0.14
Aluminum										
2024-T351	73	379	469	455	0.032	558	0.28	427	655	0.065
2024-T4	73	303	476	807	0.2	634	0.43	441	655	0.08
7075-T6	71	469	579	827	0.11	745	0.41	524	655	0.19

Table 1: Typical values of monotonic properties $\{E, \sigma_y, \sigma_{TS}, K, n, \sigma_f, \epsilon_f\}$, and cyclic properties $\{\sigma'_y, K', n'\}$ for some ductile metallic materials.

Cyclic Stress-Strain Behavior

The cyclic stress-strain response of metals is usually obtained by cycling cylindrical specimens between certain maximum and minimum imposed axial strain levels. The stress-strain response observed during cyclic straining is quite different from that observed in monotonic straining, and, depending on the initial state of the material and the testing conditions, a material may (i) cyclically harden, (ii) cyclically soften, (iii) be cyclically stable, or (iv) soften *or* harden, depending on the strain range.

Image removed due to copyright considerations.

Source: Figure 2.7 in Bannantine, Comer and Handrock. *Fundamentals of Metal Fatigue Analysis*. Englewood Cliffs, NJ: Prentice-Hall, 1990. ISBN: 013340191X.

Figure 4: Schematic of stress-strain behavior for cyclic hardening: (a) Constant strain amplitude. (b) Stress response. (c) Stress-strain response.

Image removed due to copyright considerations.

Source: Figure 2.8 in Bannantine, Comer and Handrock. *Fundamentals of Metal Fatigue Analysis*. Englewood Cliffs, NJ: Prentice-Hall, 1990. ISBN: 013340191X.

Figure 5: Schematic of stress-strain behavior for cyclic softening: (a) Constant strain amplitude. (b) Stress response. (c) Stress-strain response.

Figure 4 schematically shows **cyclic hardening behavior**. The total strain, ϵ , is cycled between equal and opposite limits ϵ^+ (positive) and $\epsilon^- (= -\epsilon^+)$ (negative), as shown in Figure 4(a). The stress response to this strain cycling is shown in Figure 4(b). The cyclic σ - ϵ behavior shown in Figure 4(c) is obtained by cross-plotting Figure 4(a) and Figure 4(b) to eliminate “time”. As seen in Figure 4(c), the stress required to enforce the strain range increases on subsequent reversals — this is called **cyclic hardening** response.

Figure 5 shows the schematic response for a material which undergoes **cyclic softening**. The stress required to enforce the strain excursions decreases with subsequent reversals.

The underlying physical reason for materials to harden or soften during cyclic straining appears to be related to the nature and stability of the dislocation substructures in metallic materials. Qualitatively speaking,

1. For a material which is **initially soft**, say due to an annealing heat treatment, the initial dislocation density is low, and during cyclic plastic straining, it increases rapidly. This increase in dislocation density causes a cycle-dependent strengthening termed **cyclic hardening**.
2. For a material which is **initially hard**, say, due to prior cold-work, the initial dislocation density is high, and during cyclic straining the rearrangement and annihila-

tion of dislocation substructures causes the overall dislocation density to decrease. This decrease in dislocation density causes a cycle-dependent loss of strength termed **cyclic softening**.

The **cyclic stress amplitude** for either type of material, often saturates to an essentially constant value after a number of strain reversals. The **stable cyclic behavior** of metals can be described in terms of amplitude-dependent [\sim stable] stress-strain hysteresis loops, as illustrated in Fig. 6.

Image removed due to copyright considerations.

Figure 6: Schematic of a stable stress-strain hysteresis loop.

With respect to this figure, the quantities

$$\Delta\epsilon, \quad \Delta\epsilon^e, \quad \text{and} \quad \Delta\epsilon^p$$

denote the **total strain range**, the **elastic strain range**, and the **plastic strain range**, respectively. Referring again to 6, it is clear that the total strain range can be additively decomposed as the sum of the elastic and plastic strain ranges,

$$\Delta\epsilon = \Delta\epsilon^e + \Delta\epsilon^p,$$

and that the elastic strain range, $\Delta\epsilon^e$, is related to the stress range, $\Delta\sigma \equiv \sigma_{\max} - \sigma_{\min}$, by

$$\Delta\epsilon^e = \frac{\Delta\sigma}{E},$$

where E is the Young's modulus. Let

$$\epsilon_a \equiv \frac{\Delta\epsilon}{2}, \quad \epsilon_a^e \equiv \frac{\Delta\epsilon^e}{2}, \quad \text{and} \quad \epsilon_a^p \equiv \frac{\Delta\epsilon^p}{2},$$

define the **strain amplitude**, the **elastic strain amplitude** and the **plastic strain amplitude**, respectively. Then, with the **stress amplitude** $\sigma_a \equiv \Delta\sigma/2$, the additive decomposition of strain amplitude can be written as

$$\boxed{\epsilon_a = \frac{\sigma_a}{E} + \epsilon_a^p.} \tag{10}$$

In order to construct a **cyclic stress-strain curve**, the tips of the stabilized hysteresis loops from comparison specimen tests at varying controlled strain amplitudes $\epsilon_a = \epsilon_1, \epsilon_2, \epsilon_3, \text{etc.}$ are connected as illustrated in Fig. 7. Note that, from the symmetry about

Image removed due to copyright considerations.

Figure 7: Construction of a cyclic stress-strain by joining tips of stabilized hysteresis loops.

the origin of the stable hysteresis loops, an identical (mirror image) cyclic-stress-strain

curve could be constructed from the compressive tips of the hysteresis loops, and the (extended) cyclic stress-strain curve would have the same symmetry in “tension” and “compression” as shown by monotonic stress-strain curves.

The cyclic stress-strain curve of a material can be compared to its monotonic stress-strain curve in order to quantitatively assess cyclically-induced changes in mechanical behavior, as illustrated schematically in Fig. 8.

Images removed due to copyright considerations.

(i)

(ii)

Figure 8: (i) Schematic comparisons of monotonic and cyclic stress-strain curves illustrating (a) cyclic softening, (b) cyclic hardening, (d) cyclically stable, and (d) mixed behavior. (ii) Monotonic and cyclic stress-strain curves for selected materials.

With respect to a cyclic stress-strain curve, the quantity σ'_y defines a **cyclic yield strength** (corresponding to a cyclic plastic strain amplitude of $\epsilon_a^p = 0.002$). And in a manner analogous to that for the monotonic stress-strain curve, a constitutive connection between the cyclic stress amplitude, σ_a , and the cyclic plastic strain amplitude, ϵ_a , can be given in power-law form, similar to equation (4), by

$$\epsilon_a^p = \left(\frac{\sigma_a}{K'} \right)^{1/n'}, \quad \text{or} \quad \sigma_a = K' (\epsilon_a^p)^{n'}, \quad (11)$$

where K' is the **cyclic strength coefficient** and n' is the **cyclic strain hardening exponent**. Substituting equation (11) into equation (10), the cyclic stress-strain curve may be summarized by

$$\epsilon_a = \frac{\sigma_a}{E} + \left(\frac{\sigma_a}{K'} \right)^{1/n'}. \quad (12)$$

Typical values of the cyclic properties $\{\sigma'_y, K', n'\}$ for some metallic materials are listed in Table 1. The value of n' varies between 0.1 and 0.2, with an average value very close to $0.15 = n'$. In general, metals with high monotonic strain hardening exponents ($n > .15$) will cyclically harden, while those with low monotonic exponents ($n < .15$) will cyclically soften. With regard to these last observations, it is perhaps appropriate to note also that initially soft materials often have high monotonic strain hardening exponents ($n > .15$), while initially hardened materials are often unable to display much additional hardening under monotonic deformation, and thus have low monotonic strain hardening exponents ($n < .15$).

As is clear from Fig. 8, it is important to note that a material which cyclically softens will have a cyclic yield strength lower than the monotonic yield strength. This points to a potential danger of using monotonic properties to predict cyclic strain amplitudes. For example, monotonic properties may predict that the strain amplitudes are fully elastic, when in fact the material may experience strain amplitudes with a substantial plastic component. As we shall see shortly, this can lead to severe consequences in terms of life predictions in fatigue.

Defect-Free Approach:

1. High-Cycle Fatigue, $N_f \gtrsim 10^4$ Cycles:

Consider a cylindrical specimen under the action of a time-varying axial stress history, $\sigma(t)$, as shown schematically in Figure 9.

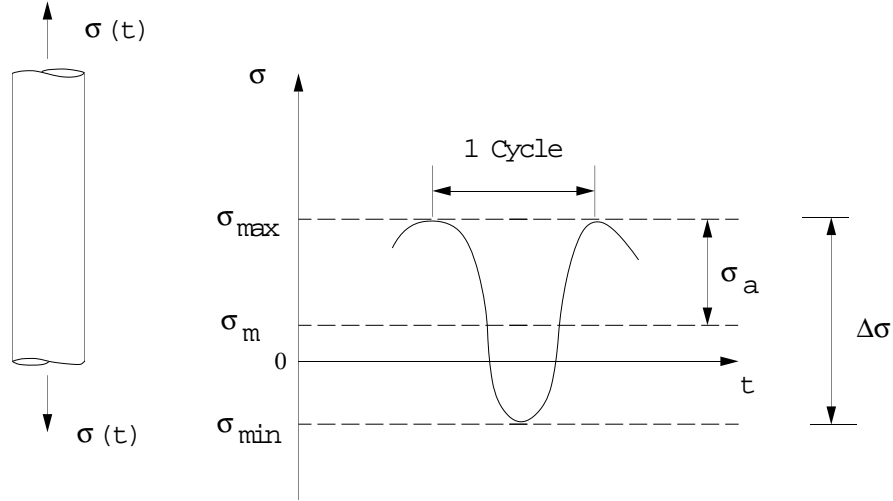


Figure 9: Fatigue testing under constant amplitude stress cycling.

With respect to this figure, the quantities

$$\begin{aligned}\Delta\sigma &= \sigma_{\max} - \sigma_{\min}, \\ \sigma_a &= \frac{\Delta\sigma}{2}, \quad \text{and} \\ \sigma_m &= \frac{1}{2}(\sigma_{\max} + \sigma_{\min})\end{aligned}\tag{13}$$

are called the **stress range**, the **stress amplitude**, and **mean stress**, respectively.

In what follows we shall first examine the relationship between the stress amplitude σ_a and the fatigue life N_f in the absence of a mean stress (i.e., when $\sigma_m = 0$), and then modify the relation for situations when a non-zero mean stress is present.

In the high-cycle fatigue regime, the stress amplitude σ_a is typically below the cyclic yield strength σ'_y of the material. The stress amplitude σ_a versus fatigue life N_f data obtained from conducting experiments at various values of σ_a are often plotted on semi-log scales, and are called **S-N curves** (S for Stress amplitude; N for Number of loading cycles to failure). Figure 10 and Figure 11 show S-N curves for the aluminum alloy 7075-T6 and for A517 steel, respectively.

Image removed due to copyright considerations.

σ_a σ_a
MPa

Figure 10: Stress amplitude σ_a versus the number of cycles to failure N_f for a 7075-T6 aluminum alloy plotted on a semi-logarithmic scale.

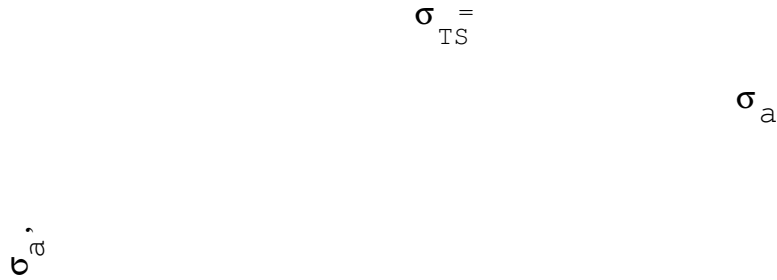


Image removed due to copyright considerations.

Figure 11: Stress amplitude σ_a versus the number of cycles to failure N_f for an A517 steel plotted on a semi-logarithmic scale.

Note that the S-N curve for the A517 steel exhibits a stress amplitude level σ_e below which the material has an apparently “infinite” fatigue life. The magnitude of the stress amplitude σ_e is called the **endurance limit** for the steel. **Most ferritic and martensitic steels exhibit an endurance limit.**

The 7075-T6 aluminum alloy, like most other non-ferrous alloys, does not show a true endurance limit. However, for engineering purposes a **pseudo-endurance limit** for non-ferrous materials is often defined as the stress amplitude corresponding to a “long” fatigue life of 5×10^6 cycles.

There is an important empirical relationship between the endurance limit, σ_e , **for wrought (not cast!) steels**, and the ultimate tensile strength σ_{TS} for the material, which is obtained less-expensively from a monotonic tension test. As shown in Figure 12,

$$\sigma_e \approx \begin{cases} 0.5 \times \sigma_{TS} & \text{if } \sigma_{TS} \lesssim 200 \text{ ksi or } 1400 \text{ MPa,} \\ 100 \text{ ksi } \approx 700 \text{ MPa} & \text{if } \sigma_{TS} > 200 \text{ ksi or } 1400 \text{ MPa.} \end{cases} \quad (14)$$

In 1910, Basquin¹ observed that the σ_a versus N_f data could be effectively linearized on log-log axes. A schematic plot of $\log \sigma_a$ versus $\log(2N_f)$ is shown in Figure 13, where $2N_f$ is **the number of reversals to failure**. Note that there

¹Basquin, O. H., “The Exponential Law Of Endurance Tests,” *Am. Soc. Test. Mater. Proc.*, **10**, pp. 625-630, 1910.

Image removed due to copyright considerations.

Source: Figure 1.4 in Bannantine, Comer and Handrock. *Fundamentals of Metal Fatigue Analysis*. Englewood Cliffs, NJ: Prentice-Hall, 1990. ISBN: 013340191X.

Figure 12: Relationship between endurance limit and tensile strength for wrought steels.

are two reversals of stress (and strain) per cycle, so that a fatigue life of N_f cycles corresponds to $2N_f$ reversals of stress. The equation of the solid-line portion of Figure 13 is

$$\boxed{\sigma_a = \sigma'_f \cdot (2N_f)^b} \quad (15)$$

The material parameters σ'_f and b are high-cycle fatigue properties of a material. They are called the **fatigue strength coefficient** and the **fatigue strength exponent**, respectively. The numerical value of the fatigue strength exponent b is generally in the range $-0.05 \geq b \geq -0.12$, with $b = -0.10$ as typical. This means that a log-log plot of the S-N curve, as in Fig. 13, appears rather “flat”. This flatness has important implications for design against high-cycle fatigue failure. Our “traditional” view of a two-dimensional plot is to think of the horizontal axis as an “independent” variable, and the vertical axis as the (resulting) “dependent” variable. But such is not the case for the S-N curve: the horizontal axis (N_f) is dependent on the stress amplitude (σ_a), so the Basquin equation (15), using the typical value of $b \doteq -0.10$ might better be expressed by the inverted form

$$2N_f = \left(\frac{\sigma_a}{\sigma'_f} \right)^{1/b} \doteq \left(\frac{\sigma_a}{\sigma'_f} \right)^{-10} = \left(\frac{\sigma'_f}{\sigma_a} \right)^{10} !$$

Thus, the **high-cycle fatigue life is typically proportional to the inverse 10th power of the applied stress amplitude**, a very strong sensitivity! Given the intrinsic uncertainties in determining the “exact” value of σ_a for actual loading histories experienced in a structure, coupled with the extreme sensitivity of high-cycle fatigue life to the precise value of σ_a , it is very difficult to make accurate

predictions of any “finite” high-cycle fatigue life. Instead, typical practice is to use the S-N curve, along with a desired high-cycle fatigue life, to identify an associated “ideal” value of stress amplitude. Then, the design value of the cyclic stress amplitude in the structure is reduced from this “ideal” value by a safety factor, often in the range of a factor of 2.

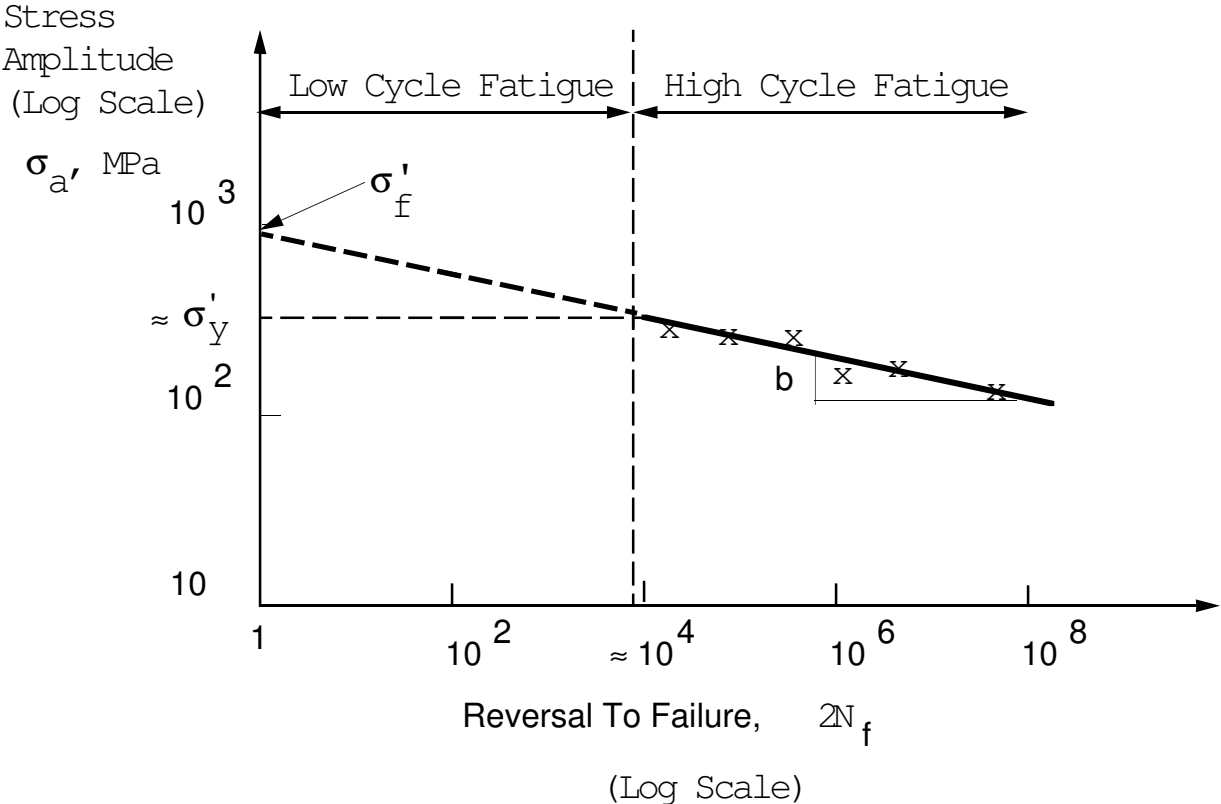


Figure 13: Schematic plot of stress amplitude σ_a versus reversals to failure ($2N_f$) for the high-cycle fatigue regime; log-log axes.

As mentioned previously, in the high-cycle fatigue regime, the stress amplitude σ_a is typically below the cyclic yield strength, σ'_y , of the material, and this produces small stabilized hysteresis loops, Figure 14. The area within the loop is the energy per unit volume dissipated as plastic work during a cycle. In the high-cycle regime, this energy dissipation (loss) is small, and it decreases rapidly as the stress amplitude decreases. However, if the imposed stress amplitude increases beyond the cyclic yield strength σ'_y , then the cyclic plastic strain amplitude and the width of the stabilized hysteresis loops rapidly become large, and the resulting fatigue life typically decreases to below $\approx 10^4$ cycles. We discuss the case of low-cycle fatigue next.

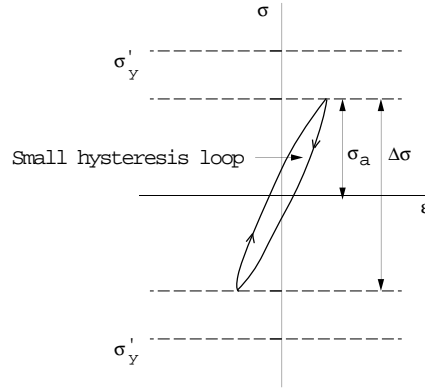


Figure 14: Schematic of a small hysteresis loop produced in the high-cycle regime when the stress amplitude σ_a is typically less than the monotonic yield strength σ_y of the material.

2. Low-Cycle Fatigue, $N_f \lesssim 10^4$ Cycles:

Figure 15 shows a schematic of a hysteresis loop in the low-cycle regime. With respect to this figure, the quantities

$$\Delta\epsilon, \quad \Delta\epsilon^e, \quad \text{and} \quad \Delta\epsilon^p$$

denote the **total strain range**, the **elastic strain range**, and the **plastic strain range**, respectively. Again,

$$\Delta\epsilon = \Delta\epsilon^e + \Delta\epsilon^p, \quad \text{with} \quad \Delta\epsilon^e = \frac{\Delta\sigma}{E},$$

where $\Delta\sigma$ is the stress range, and E is the Young's modulus. Let

$$\epsilon_a = \frac{\Delta\epsilon}{2}, \quad \epsilon_a^e = \frac{\Delta\epsilon^e}{2}, \quad \text{and} \quad \epsilon_a^p = \frac{\Delta\epsilon^p}{2},$$

denote the **strain amplitude**, the **elastic strain amplitude** and the **plastic strain amplitude**, respectively. Then, as before,

$$\boxed{\epsilon_a = \frac{\sigma_a}{E} + \epsilon_a^p.} \quad (16)$$

In the mid-1950's, Coffin² and Manson³ independently established a power law correlation for the low-cycle fatigue life, N_f , with the cyclic plastic strain amplitude,

²Coffin, L. F., "A study of the Effects of Cyclic Thermal Stresses on a Ductile Metal," *Trans ASME*, **76**, 1954, pp. 931 - 950.

³Manson, S. S., "Behavior of Materials under Conditions of Thermal Stress," *Heat Transfer Symposium*, University of Michigan Engineering Research Institute, 1953, pp. 9 - 75.

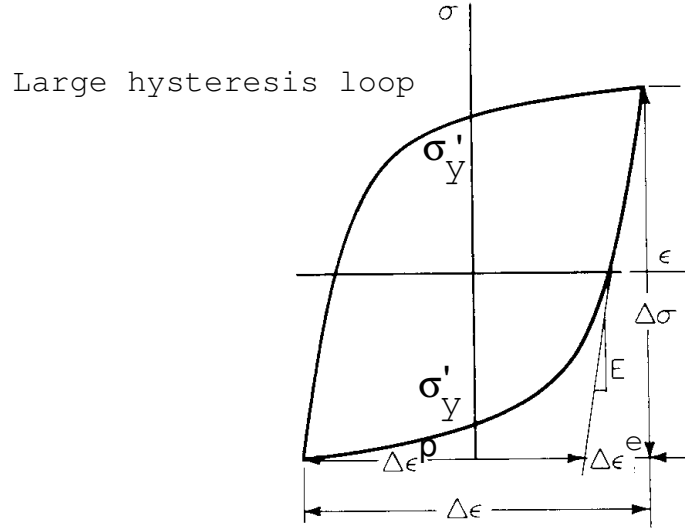


Figure 15: Schematic of a large hysteresis loop produced in the low-cycle regime when the stress amplitude σ_a is typically larger than the monotonic yield strength σ_y of the material.

ϵ_a^p , as shown in Figure 16. The straight line on this log-log plot has the equation

$$\boxed{\epsilon_a^p = \epsilon'_f (2N_f)^c} \quad (17)$$

The material parameters ϵ'_f and c are the low-cycle fatigue properties for a material. They are called the **fatigue ductility coefficient** and the **fatigue ductility exponent**, respectively. Numerical values of the fatigue ductility exponent are usually in the range $-0.5 \geq c \geq -0.7$ for many metals, with $c = -0.6$ as typical. Note that this dependence of low-cycle fatigue life on plastic strain amplitude, when inverted, is more robust than in the case of high-cycle fatigue, leading to

$$2N_f = \left(\frac{\epsilon_a^p}{\epsilon'_f} \right)^{1/c} = \left(\frac{\epsilon_a^p}{\epsilon'_f} \right)^{-5/3} = \left(\frac{\epsilon'_f}{\epsilon_a^p} \right)^{5/3}.$$

In low-cycle fatigue, fatigue life is proportional to plastic strain amplitude to the inverse ~ 1.67 power. This level of sensitivity is sufficiently small so that small differences in ϵ_a^p (from those assumed) lead to meaningfully small differences in resulting predictions of low-cycle fatigue life.

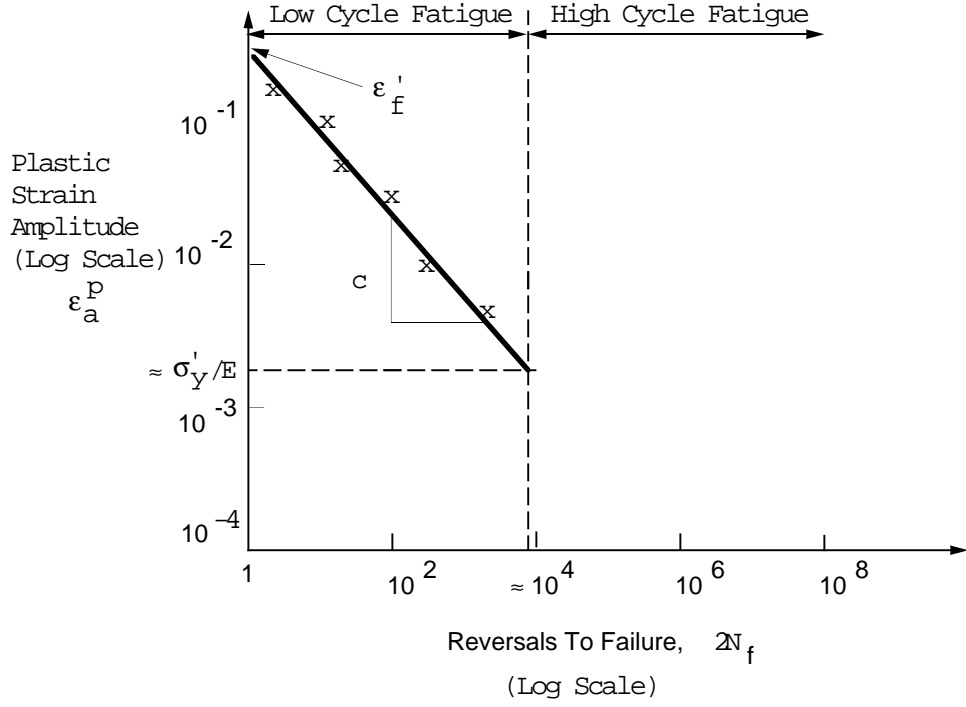


Figure 16: Schematic plot of strain amplitude ϵ_a versus reversals to failure ($2N_f$) for low-cycle fatigue on log-log axes.

3. Strain-Life Equation for both High-Cycle and Low-Cycle Fatigue:

We can now combine the equation of the cyclic strain amplitude, equation (16) with the fatigue life correlations for the high-cycle regime, equation (15), and for the low-cycle regime equation (17) to obtain

$$\epsilon_a = \underbrace{\frac{\sigma'_f}{E}(2N_f)^b}_{\epsilon_a^e} + \underbrace{\epsilon'_f(2N_f)^c}_{\epsilon_a^p}. \quad (18)$$

Equation (18) is the basis for the strain-life approach to design against fatigue failure. The strain-life equation is shown schematically in Figure 17 as being asymptotic to the two straight lines corresponding to equations (15) and (17) at long and short lives, respectively.

Also indicated in Figure 17 is the **transition fatigue life**, $2N_t$. It is the life at which the cyclic elastic strain range equals the cyclic plastic strain range. Dividing (15) by E to obtain ϵ_a^e and setting this equal to ϵ_a^p , equation (17), we obtain that

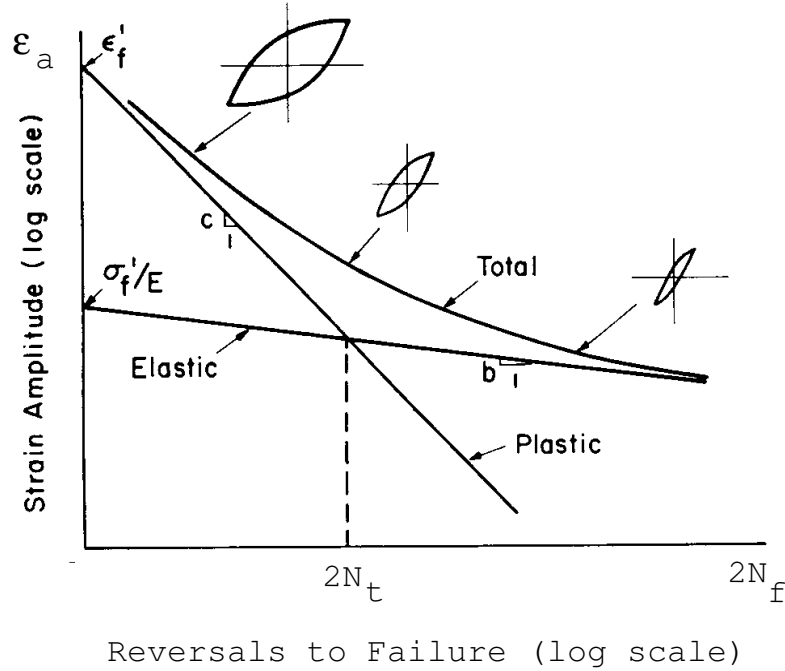


Figure 17: Schematic plot of elastic, plastic and total strain amplitudes versus reversals to failure ($2N_f$). The **transition** number of reversals at which the elastic strain amplitude equals the plastic strain amplitude is denoted by ($2N_t$). Shapes of hysteresis curves in relation to the strain-life curve are also shown.

the transition fatigue life is given by the expression

$$2N_t = \left\{ \frac{E \epsilon'_f}{\sigma'_f} \right\}^{\frac{1}{(b-c)}}. \quad (19)$$

At short lives, $2N_f < 2N_t$, plastic strain will predominate, and ductility will control the fatigue performance. At long life, $2N_f > 2N_t$, the plastic strain will be far smaller than the elastic strain, and strength will control the fatigue performance.

It is important to take note of the tradeoffs inherent in material selection to design against high-cycle and low-cycle fatigue. An examination of the tables shows that, as a general trend, the fatigue strength coefficient, σ'_f correlates positively with measures of a material's resistance to monotonic plastic deformation such as tensile yield strength, σ_y , or hardness; consequently, standard approaches to improving high-cycle fatigue performance have involved material compositions and processing means to increase strength, including use of alloying elements, heat-treating, and special surface-hardening treatments (e.g., carburizing, nitriding, etc.). However,

we recall from our previous examinations of elastic-plastic materials that, in general, increases in strength are invariably accompanied by decreases in ductility, or monotonic true strain at fracture. And these associated reductions in the material's ability to undergo plastic deformation without fracture under monotonic loading also manifest themselves in a corresponding decrease in its fatigue ductility coefficient, ϵ'_f . Reduced values of the latter material property mean that lower fatigue lives will result from application of any given value of plastic strain range, ϵ_a . This trend in overall strain amplitude/fatigue life response, as a function of hardness in various quenched and tempered states of alloy steel 4142 are shown in the table below.

Brinnell Hardness (<i>HB</i>)	σ'_f (MPa)	b	ϵ'_f	c
670 (as-quenched)	2550	-0.0778	0.0032	-0.436
560	2410	-0.121	0.0732	-0.805
450	1937	-0.0762	0.706	-0.869

Table 2: Typical values of fatigue strength and ductility properties for differing tempers (and hence hardnesses) of quenched and tempered 4142 steel.

Material	Endurance Limit	Strain-Life Properties			
	σ_e MPa ($N_f = 5 \times 10^6$)	σ'_f MPa	b	ϵ'_f	c
Steel					
SAE 1020 (hot rolled)	152	896	-0.12	0.41	-0.51
SAE 1040 (As forged)	173	1540	-0.14	0.61	-0.57
Man-Ten (hot rolled)	262	1089	-0.115	0.86	-0.65
RQC-100 (hot rolled)	403	938	-0.0648	0.66	-0.69
SAE 4340 (Q & T)	492	1655	-0.076	0.73	-0.62
Aluminum					
2024-T351	151	1100	-0.124	0.22	-0.59
2024-T4	175	1015	-0.11	0.21	-0.52
7075-T6	176	1315	-0.126	0.19	-0.52

Table 3: Typical values of fatigue properties $\{\sigma_e, \sigma'_f, b, \epsilon'_f, c\}$ for some ductile metallic materials. Note that the “endurance limit” σ_e in this table is a pseudo-endurance limit, which is calculated from Basquin’s relation for a life of $N_f = 5 \times 10^6$ cycles.

Mean Stress Effects on Fatigue

The preceding section described relations between stress, plastic strain, and total strain amplitudes and the corresponding fatigue life under conditions of fully reversed loading with zero mean stress. We take the mean stress associated with a cyclic loading between stress limits σ_{\max} and σ_{\min} to be $\sigma_m = (\sigma_{\max} + \sigma_{\min})/2$, with cyclic amplitude $\sigma_a = (\sigma_{\max} - \sigma_{\min})/2$. Mean stress effects on fatigue life are most important at long lives, where cyclic plastic straining is small. At low lives, with significant plastic straining, mean stresses quickly relax out under strain-controlled limits, or lead to cyclic ratcheting and “run-away” if it is attempted to enforce unequal stress limits. Although many design approaches have been proposed to account for long-life mean stress effects on fatigue, we will adopt the assumption that a tensile mean stress, $\sigma_m > 0$, will correspondingly reduce the effective fatigue strength coefficient of eq. (15). The modified form of the Basquin relation then becomes

$$\sigma_a = (\sigma'_f - \sigma_m) \cdot (2N_f)^b; \quad (\text{for } \sigma_m > 0). \quad (20)$$

When this equation is inserted into eq. (18), the governing equation for the strain-life approach is as

$$\epsilon_a = \left(\frac{\sigma'_f - \sigma_m}{E} \right) \cdot (2N_f)^b + \epsilon'_f \cdot (2N_f)^c, \quad (21)$$

The effect of a positive mean stress on the strain-life curve is to reduce the long-life asymptote by σ_m/E . If the mean stress was compressive, $\sigma_m < 0$, then the use of eq. (21) rather than eq. (18), would predict that the long-life fatigue behavior would considerably **exceed** that obtained under conditions of zero mean stress. While there are indications that this interpretation of the “beneficial” effects of compressive mean stress on long-life fatigue performance has a degree of validity, a conservative approach would be to continue to use eq. (18) rather than eq. (21) (and eq. (15) rather than eq. (20)) in those cases where σ_m is negative.

Cumulative Fatigue Damage

The strain-life relations developed in the preceding sections are for **constant amplitude straining** throughout the fatigue life of the member. In order to apply information of this type to the analysis of the fatigue behavior of structural elements which are subjected to other than uniform cyclic straining, it is necessary to develop a formalism for generalization of constant amplitude life data to variable amplitude loading.

The earliest, and still most successful, such generalizing concept in defect-free fatigue analysis is that of *cumulative fatigue damage*, first introduced by Palmgren and by Miner.

In order to motivate the procedure, consider a simple two-stage cyclic straining history consisting of n_1 cycles of strain amplitude $\epsilon_{a(1)}$, followed by application of a different strain amplitude, $\epsilon_{a(2)}$, until failure occurs. We wish to determine the number of cycles, n_2 , of the second strain amplitude which can be applied before fatigue failure occurs.

Let N_{f1} be the number of cycles to failure for constant amplitude straining $\epsilon_{a(1)}$. Obviously, in the present problem the parameter

$$d_1 \equiv \frac{n_1}{N_{f(1)}} \quad (22)$$

satisfies $d_1 \leq 1$. We call d_1 the “damage” which the material has undergone during the application of the first loading block. We generalize this concept of damage and denote by “ d_i ” the damage associated with the “ i -th” portion of the loading history, consisting of n_i cycles of strain range $\Delta\epsilon_i$ (strain amplitude $\epsilon_{a(i)}$). Under constant amplitude conditions, this strain range would result in a fatigue life of $N_{f(i)}$ cycles (or $2N_{f(i)}$ reversals). The “ i -th” damage increment is then defined by

$$d_i \equiv \frac{n_i}{N_{f(i)}} (0 \leq d_i \leq 1). \quad (23)$$

The theory of *linear cumulative fatigue damage* assumes that fatigue failure occurs when

$$\sum_i d_i = \sum_i \frac{n_i}{N_{fi}} = 1. \quad (24)$$

(Note that the application of eq. (24) to any constant amplitude history will trivially reproduce the baseline strain-life curve, as it should.)

In our example problem, where the number of blocks was two (2), the application of eq. (24) provides

$$\sum_{i=1}^2 d_i = \frac{n_1}{N_{f1}} + \frac{n_2}{N_{f2}} = 1.$$

Or, on rearranging, to solve for the unknown number (n_2) of cycles of strain amplitude $\epsilon_{a(2)}$ that can be applied subsequent to the previously-applied n_1 cycles of strain amplitude $\epsilon_{a(1)}$ before fatigue failure results as

$$n_2 = N_{f2} \cdot \left[1 - \frac{n_1}{N_{f1}}\right].$$

One important limitation of the cumulative damage rule as presented here is that there is no explicit accounting for sequence effects on fatigue. That is, n_2 cycles of strain amplitude $\epsilon_{a(2)}$, followed by n_1 cycles of strain amplitude $\epsilon_{a(1)}$, would also satisfy eq. (24), but due to various features of the cyclic stress-strain curve, the gradual change (via cyclic hardening or softening) from the monotonic to the cyclic stress-strain curve, and other factors, there can be a block sequence effect on fatigue life. These effects can be accounted for to some degree in sophisticated computer-based applications of cumulative damage which break arbitrary loading histories into single, sequential reversals, and which simultaneously follow the cyclic stress-strain curve along each segment of the loading history. These developments are beyond the scope of this course.

NOTCH EFFECTS ON FATIGUE

We have developed certain tools for implementing a defect-free fatigue life methodology based primarily on the local strain approach to fatigue. Thus far, however, we have considered only small cylindrical specimens or components subjected to uniaxial cyclic loading. In practice, crack initiation and fatigue failure in components of more complex geometry are most often associated with stress concentrations arising at notches, holes, fillets, radii, and other necessary geometrical discontinuities.

An intuitive notion why this should be so can be gleaned from the long-life fatigue behavior of a notched component. If the cyclic loadings are sufficiently small so that negligible cyclic plastic strain occurs within the body, we may expect that the theory of elasticity can be used to calculate stress, strain and displacement.

Consider the elliptical hole of major and minor axes ($2a$, $2b$), respectively, located in a large body subject to the far-field cyclic fully-reversed nominal stress amplitude S_a , normal to the $2a$ direction. The local stress amplitude occurring at the root of the notch, $\sigma_a \equiv \sigma_{a(\text{local})}$, can be obtained from the equations of elasticity as

$$\sigma_a = (1 + 2\sqrt{a/\rho}) \cdot S_a \equiv K_t \cdot S_a \quad (25)$$

Here $\rho = b^2/a$ is the radius of curvature at the notch root of the ellipse, and the dimensionless quantity $K_t \geq 1$ is the *stress concentration factor*. A wide variety of elastic stress concentration factors for practical engineering geometries can be found in the handbook **Stress Concentration Factors**, by R. E. Petersen.

For long-life fatigue of laboratory-sized uniaxial [homogeneously-stressed] specimens, the Basquin stress/life fatigue correlation of eq. (15) gives:

$$\sigma_a = \sigma'_f \cdot (2N_f)^b \quad (15a)$$

or

$$2N_f = (\sigma_a/\sigma'_f)^{1/b}, \quad (15b)$$

where σ'_f , the fatigue strength coefficient, and b , the fatigue strength exponent, are material properties, and $2N_f$ is the number of reversals to failure under a fully-reversed applied stress amplitude of magnitude σ_a .

Since, as noted previously, $0 > b \simeq -1$, typically, we see that (long) fatigue life is a very sensitive function of stress amplitude — proportional roughly to the inverse tenth power. Thus, if we imagine a small material coupon at the notch root where, from

eq. (25), the local stress amplitude is greater than at remote locations, it should come as no surprise that fatigue failure invariably starts at the stress concentration of a notch root.

An operational definition of the severity of a given notch, in a given material, in reducing the long-life fatigue strength of the structure, S_e , can be given in terms of the *fatigue notch factor*, K_f . Here S_e is the fully-reversed nominal stress amplitude which may be applied to the notched component with a resulting fatigue life of some arbitrary, but specified, number of cycles. Often this “long” life (or nominal stress “endurance” limit) is chosen as $2N_f = 10^7$ reversals (or $N_f = 5 \times 10^6$ cycles). Let S_f be defined as the stress amplitude resulting in the same fatigue life for the material, but in a uniaxially-loaded specimen. From eq. (15a),

$$S_f = \sigma'_f \cdot (10^7)^b$$

or

$$10^7 = (S_f/\sigma'_f)^{1/b}$$

The **notch fatigue factor**, K_f , is defined as the ratio of long life uniaxial stress amplitude for long-life notched stress amplitude:

$$K_f \equiv \frac{S_f}{S_e}. \quad (26)$$

We expect that the notched fatigue strength, phrased in terms of the nominal stress amplitude, will not exceed the unnotched fatigue strength, and so we expect $K_f \geq 1$. A theoretical value for K_f can be obtained by hypothesizing that:

- (a) in order to obtain a notch fatigue life of $2N_f = 10^7$, the *local* stress amplitude at the notch root will be $\sigma_a = S_f$.
- (b) the elastic stress concentration factor K_t relates nominal stress $S_a = S_\ell$ to the local stress $\sigma_a = S_f$ by

$$S_f = K_t \cdot S_e$$

or

$$S_e = S_f/K_t.$$

When this last expression is inserted into eq. (26), there results the prediction:

$$\begin{aligned} K_f^{(\text{predicted})} &= S_f/S_\ell \\ &= S_f/(S_f/K_t) \\ &= K_t. \end{aligned} \tag{27}$$

This prediction is generally good, and conservative in the sense that experimentally-observed values for K_f satisfy $K_t \geq K_f \geq 1$. The limiting value of $K_{f(\text{max})} = K_t$ is generally associated with:

- (a) “higher”-strength materials, and
- (b) “larger” notch root radii, ρ .

One notion which can help to suggest reasons why we can obtain $K_f < K_t$ is the stress gradient at the notch. The highest theoretically-predicted stresses are experienced only by a vanishingly thin lamina of material on the surface of the notch, and material points in the bulk at any finite distance below the notch root experience less severe cyclic stressing.

We presume that in notch fatigue, a critical value of fatigue damage must be sustained over material volume elements possessing some characteristic “microstructural” linear dimension, ρ^* . This assumption can provide qualitative insight as to the dependence of K_f on K_t , root radius, ρ , and a “material” length-scale, ρ^* . For example, higher-strength materials are often associated with refinement of microstructural dimensions such as grain size, free length of dislocation segment between pinning points, etc. (recall the aphorism ‘smaller is stronger’ in understanding plastic resistance of polycrystalline metals) Thus, we might expect higher-strength materials to have generally smaller values of ρ^* . On dimensional grounds, we also expect K_f to depend on K_t and on the *ratio* ρ^*/ρ . One empirical expression for K_f which was fitted by Petersen to notch fatigue data for wrought steels of varying strength is:

$$K_f = 1 + \frac{K_t - 1}{1 + \rho^*/\rho}, \tag{28}$$

where the material length scale ρ^* depends inversely on the monotonic tensile strength, σ_{TS} , according to

$$\rho^* = \rho_0 \cdot \left(\frac{\sigma^*}{\sigma_{TS}}\right)^{1.8}. \tag{29}$$

In eq. (29), the [constant] reference length ρ_0 and reference stress level σ^* are given for wrought steels by

$$\rho_0 = .001 \text{ in} = 25.4 \times 10^{-6} m$$

$$\sigma^* = 300 \text{ ksi} = 2070 \text{ MPa},$$

and σ_{TS} is the tensile strength for the material at hand.

Typical values for ρ^* in steels of various conditions are:

Material Condition	Typical ρ^*
Annealed, normalized steels	.01" = 0.25 mm
Quenched and tempered steels	.025" = 0.1 mm
Highly-hardened steels	.001" = 0.025 mm

Returning to eq. (28)), we see that for $\rho^*/\rho \ll 1$, $K_f \simeq K_t$, while for $\rho^*/\rho \gg 1$, $K_f \simeq 1$. The inflection point in the curve of K_f vs. ρ^*/ρ occurs for root radii $\rho \simeq \rho^*$.

To summarize the high-cycle fatigue approach to notch roots in wrought steels, we apply the following steps:

Step 1 Using the material's tensile strength, σ_{TS} , calculate its characteristic length scale, ρ^* , from eq. (29).

Step 2 Using the theoretical elastic stress concentration factor, K_t , for the notch geometry, calculate the notch fatigue factor, K_f , from its root radius, ρ , and the material length scale ρ^* , using eq. (28).

Step 3 Calculate the nominal stress amplitude, S_a , giving high-cycle fatigue failure of the notched component in N_f cycles (or $2N_f$ reversals) according to

$$\boxed{K_f S_a = \sigma'_f \cdot (2N_f)^b.} \quad (30)$$

Fatigue Stress and Strain Concentration Factors

The previous discussion of notches in fatigue assumed that cyclic elastic behavior occurs not only remotely, in response to the nominal stress amplitude, S_a , but also locally (at the notch root), in response to the local cyclic stress amplitude, σ_a . While this will be true for sufficiently small amplitudes of cyclic loading, it is also possible for cyclic plasticity to occur. With this in mind, we introduce the (notch root) strain amplitude, ϵ_a , (corresponding to σ_a on the cyclic stress-strain curve) and the nominal strain amplitude, e_a , analogously corresponding to S_a . We define the **cyclic stress concentration factor**, K_σ , as:

$$K_\sigma \equiv \frac{\sigma_a}{S_a} \quad (31)$$

and the **cyclic strain concentration factor**, K_ϵ , as

$$K_\epsilon \equiv \frac{\epsilon_a}{e_a}. \quad (32)$$

In the case of cyclic elastic deformation, both at the notch root in response to σ_a , and in the nominal stress/strain relation,

$$S_a = E e_a; \quad \sigma_a = E \epsilon_a,$$

so that $K_\sigma = K_\epsilon = K_t$.

When the local notch fields exhibit cyclic plastic behavior, we generally find that

$$K_\sigma < K_t;$$

$$K_\epsilon \geq K_t.$$

One means for accounting for effects of notch root plasticity is the use of **Neuber's rule**:

$$K_\sigma \cdot K_\epsilon = (K_t)^2 \quad (33)$$

Eq. (33) can be shown to be rigorously correct for certain cases of notch root elastic-plastic behavior, as initially shown in solutions due to H. Neuber. In applications of this result to notch fatigue problems (anticipating notch fatigue life correlations) it is common to replace “ K_t ” with the fatigue notch factor, K_f , giving

$$K_\sigma \cdot K_\epsilon = (K_f)^2 \quad (34)$$

or, in view of eq. (31) and eq. (32),

$$(\sigma_a/S_a) \cdot (\epsilon_a/e_a) = (K_f)^2 \quad (35)$$

or, on further arrangement,

$$\sigma_a \cdot \epsilon_a = S_a \cdot e_a \cdot (K_f)^2 \quad (36)$$

When the nominal stress amplitude is within the cyclic elastic limit, $S_a < \sigma'_y$, then $e_a = S_a/E$ and

$$\sigma_a \cdot \epsilon_a = \frac{(S_a \cdot K_f)^2}{E}. \quad (37)$$

We can insert the equation for the cyclic stress/strain curve,

$$\epsilon_a = \frac{\sigma_a}{E} + \left(\frac{\sigma_a}{K'}\right)^{1/n'}, \quad (12)$$

into eq. (37) to obtain

$$\sigma_a^2 + E\sigma_a \cdot \left(\frac{\sigma_a}{K'}\right)^{1/n'} = (S_a \cdot K_f)^2. \quad (38)$$

For prescribed geometry, material, and loading, both K_f and S_a can be determined. Eq. (38) can then be solved iteratively for the resulting notch root stress amplitude, σ_a . With σ_a known, the notch root strain amplitude, ϵ_a , can be determined by substituting the value of σ_a into eq. (12). Finally, with the known local strain amplitude, ϵ_a , the notch fatigue life $2N_f$ is obtained from the strain life curve as

$$\epsilon_a = \epsilon'_f \cdot (2N_f)^c + \left(\frac{\sigma'_f}{E}\right) \cdot (2N_f)^b.$$

It is important to note that a critical step in the overall methodology was the use of Neuber's rule in the form of eqs. (36) and (37) to obtain relations between local and nominal cyclic loadings. Generally, Neuber's rule is most appropriate for planar geometries in generalized plane stress with root radius ρ of comparable size with sheet thickness t : $\rho \geq \sim t$. The use of Neuber's rule for notch roots in more triaxial states of stress, (e.g., in planar geometries with $\rho < t$) is generally conservative in that the

notch fatigue life tends to be underestimated. A different (and easier to use) connection between local and nominal fields which is more appropriate for small ρ/t or for axial symmetry is the so-called “**linear rule**”:

$$K_\epsilon = K_f \tag{39}$$

resulting in

$$\frac{\epsilon_a}{e_a} = K_f \tag{40}$$

or

$$\epsilon_a = K_f \cdot e_a. \tag{41}$$

For elastic response to the nominal stressing, $e_a = S_a/E$, and the linear rule gives the notch strain amplitude as

$$\boxed{\epsilon_a = K_f \cdot \frac{S_a}{E}} \tag{42}$$

Notch fatigue life for this class of notches is also obtained by substituting the local strain ϵ_a determined from eq. (42) into the strain/life correlation of eq. (18). The cyclic strain determined from eq. (42) will generally be smaller than that obtained from eqs. (20) and (19), so that somewhat different lives are predicted.